JOURNAL OF BACTERIOLOGY, Dec. 1998, p. 6364–6374 Vol. 180, No. 23
0021-9193/98/$04.00+0

Effects of Chromosome Underreplication on Cell Division in *Escherichia coli*

EMILIA BOTELLO† AND KURT NORDSTRÖM*

Department of Microbiology, Biomedical Center, Uppsala University, S-751 23 Uppsala, Sweden

Received 5 May 1998/Accepted 30 September 1998

The key processes of the bacterial cell cycle are controlled and coordinated to match cellular mass growth. We have studied the coordination between replication and cell division by using a temperature-controlled *Escherichia coli intR1* strain. In this strain, the initiation time for chromosome replication can be displaced to later (underreplication) or earlier (overreplication) times in the cell cycle. We used underreplication conditions to study the response of cell division to a delayed initiation of replication. The bacteria were grown exponentially at 39°C (normal DNA/mass ratio) and shifted to 38 and 37°C. In the last two cases, new, stable, lower DNA/mass ratios were obtained. The rate of replication elongation was not affected under these conditions. At increasing degrees of underreplication, increasing proportions of the cells became elongated. Cell division took place in the middle in cells of normal size, whereas the longer cells divided at twice that size to produce one daughter cell of normal size and one three times as big. The elongated cells often produced one daughter cell lacking a chromosome; this was always the smallest daughter cells, and it was the size of a normal newborn cell. These results favor a model in which cell division takes place at only distinct cell sizes. Furthermore, the elongated cells had a lower probability of dividing than the cells of normal size, and they often contained more than two nucleoids. This suggests that for cell division to occur, not only must replication and nucleoid partitioning be completed, but also the DNA/mass ratio must be above a certain threshold value. Our data support the ideas that cell division has its own control system and that there is a checkpoint at which cell division may be abolished if previous key cell cycle processes have not run to completion.

The cell cycles of all organisms contain key events that occur only once during each doubling in mass, replication of the genome, separation of the daughter genomes, and cell division. These events are carefully coordinated with each other and controlled to match the increase in cell mass. In eukaryotic cells, there seem to be two independent, alternating processes, genome replication (S phase) and separation of the daughter genomes (M phase); each S phase requires a preceding M phase and vice versa (27).

During the bacterial cell cycle (for reviews, see references 15, 24, 30, and 38), there are three recognized periods at a slow growth rate, B, C, and D (20). Chromosome replication occurs during period C, and nucleoid partitioning and cell division take place during period D. The length of C plus D can be much longer than the generation time, τ. To accommodate this, there may be up to three overlapping replication cycles at a rapid rate of growth. Hence, alternations between periods C and D cannot occur in bacteria as they do in eukaryotic cells. Therefore, under different growth conditions, replication initiates and partitioning occurs at different times in the cell cycle and can take place at any time from birth to cell division. Since there may be overlapping replication cycles, there cannot be a requirement for completed nucleoid partitioning before the next replication cycle is initiated. Cell division does not seem to be required for the two other key events, and thus, inhibition of cell division leads to the formation of filaments with 2, 4, 8, 16, etc., separated nucleoids. Damage to the DNA or other effects that slow down replication induce systems, such as the SOS system, that transiently delay cell division in order to allow replication to be completed before the cell divides. Inhibition of initiation of chromosome replication reduces the frequency of, but does not totally block, cell division, which leads to the formation of elongated or filament cells; the residual cell division causes the formation of DNA-less cells. This and other pieces of information indicate that initiation of chromosome replication, nucleoid partitioning, and cell division have independent control systems that link these processes to cell mass (for reviews, see references 15, 24, 30, and 38). This requires that within a single cell cycle there are checkpoints that ensure that chromosome replication is finished before nucleoid partitioning and cell division take place.

To address the questions of the number of control points in the cell cycle of *Escherichia coli* and their molecular basis, we have constructed so-called *int* strains (4, 17, 23, 29). In these strains, a 16-bp deletion in the leftmost 13-mer of the chromosomal replication origin, *oriC*, which is crucial for the initial opening of the origin at initiation of replication, has inactivated *oriC* (8). Plasmid replicons have been inserted into *oriC*. Thereby, chromosome replication is controlled by the plasmid replicon and independent of the normal cell cycle controls. The copy number of plasmid R1 is about the same as that of *oriC* at moderate and high growth rates (18) and is essentially regulated by two transcription rates, that of the mRNA for the rate-limiting initiator protein (RepA) and that of the antisense RNA (CopA) that negatively controls the efficiency by which the RepA mRNA is translated (28). We have constructed *intR1* strains in which both of these transcription rates are controlled by temperature such that the chromosome content is normal at 39°C, lower (underreplication) at lower temperatures, and higher (overreplication) at temperatures above 39°C

* Corresponding author. Mailing address: Department of Microbiology, Biomedical Center, Uppsala University, Box 581, S-751 23 Uppsala, Sweden. Phone: 46 18 471 45 26. Fax: 46 18 53 03 96. E-mail: kurt.nordstroem@mikrobio.uu.se.

† Present address: Departamento de Bioquímica y Biología Molecular y Genética, Facultad de Ciencias, Universidad de Extremadura, 06080 Badajoz, Spain.

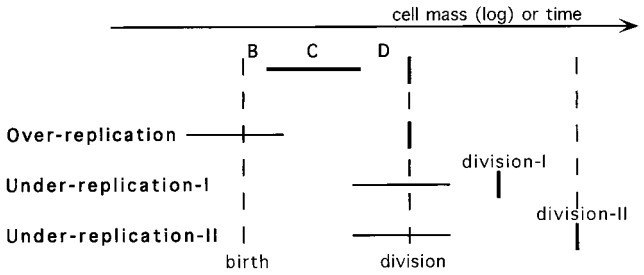

FIG. 1. Over- and underreplication during the cell cycle. B, C, and D designate the different cell cycle periods. Under-replication-I and -II, working hypotheses about the effects of chromosome underreplication on cell division.

(4, 6). This corresponds to increasing or decreasing the initiation mass, which is the same as moving the time of initiation of replication to later or earlier times in the cell cycle compared to the normal situation (see Fig. 1).

These *int* strains have been used to study how nucleoid partitioning and cell division are controlled (1–3, 5, 6, 13). By using the temperature-controlled *intR1* strains under conditions of overreplication, we have been able to show that cell division does not seem to be triggered by chromosome replication but rather that it has its own, independent means of control (3). This system was also used to switch off initiation of replication, allowing ongoing rounds of replication to proceed to completion, and afterward to switch on a single or multiple rounds of replication in order to study the correlation between chromosome replication and cell division (6). Several other groups have studied the effects on cell division of inhibition and switching on of DNA replication by using temperature-sensitive *dna* mutants (see reference 20, p. 1635 to 1636). However, with our *intR1* system, it is possible to study populations growing exponentially at reduced DNA/mass ratios, i.e., without switching off replication during the experiment. Hence, there will not be any disruption of the cell cycle, and the physiology of the cells will be less disturbed than it is in the switch-off/switch-on experiments referred to above. This allows studies of more aspects of the cell cycle, e.g., the correlation between the timing of initiation of chromosome replication and nucleoid processing-cell division, the requirement of factors other than completed replication for cell division, the causes for inhibition of cell division at increased initiation mass, and the location of cell divisions in elongated and filamented cells, etc.

We have used the *intR1* system to study the effects of underreplication (reduced DNA/mass ratio) on key cell cycle events during exponential growth. The ratio between CopA RNA and RepA mRNA sets the DNA/mass ratio at levels that deviate from the normal value. Shifts from 39°C to lower temperatures lead to exponential growth with new, reduced DNA/mass ratios, because the rate of synthesis of CopA RNA is increased. A reduction in the DNA/mass ratio corresponds to movement of initiation of replication to later-than-normal times (Fig. 1). The question of how nucleoid partitioning and cell division respond to this arises. Will the length of the D period be kept constant and the cells divide at continuously increasing sizes as the delay in replication increases ("Under-replication-I" in Fig. 1), or do the cells omit cell division and wait until they are twice the normal septating size ("Under-replication-II" in Fig. 1)? Our data are essentially in accord with the latter.

MATERIALS AND METHODS

Strains. The *E. coli* K-12 strains used in this study were EC1005 (*metB1 nalA relA1 spoT1* λ^r F^-) (19) and its *intR1* derivative EC::71CW/pOU420Ap^s (6).

Chromosome replication in the *intR1* strains is controlled by a plasmid R1 replicon, which is inserted into *oriC* (4, 23, 29). R1 replication is controlled by the RepA protein and the CopA antisense RNA. RepA is required for initiation of replication from *oriR1*, and it is rate limiting for this event, while CopA controls R1 replication by inhibiting the synthesis of RepA (28). The construction and characterization of the *intR1* strain EC::71CW/pOU420Ap^s have been described previously (6). In this *intR1* strain, the synthesis of RepA and CopA is thermodependent and CopA is produced from the R1 derivative replicon inserted into *oriC* as well as from the plasmid pOU420Ap^s. By decreasing the growth temperature a few degrees, from 39°C to 38, 37, or 36°C, increasing amounts of CopA antisense RNA and decreasing amounts of RepA protein are simultaneously produced (6).

Media and growth conditions. Bacteria were grown in M9 medium supplemented with 0.2% glucose, 50 μg of methionine per ml, and 1 μg of thiamine per ml (M9 glucose medium) (32). To EC::71CW/pOU420Ap^s cultures, 20 μg of ampicillin and 50 μg of chloramphenicol were added per ml.

The cultures were incubated in thermostatically controlled water baths (Heto) with a maximum deviation of 0.2°C from the set temperature. Growth in mass was monitored by the absorbence of the culture at 550 nm (A_{550}), using a Novaspec II spectrophotometer (LKB). Exponentially growing cultures were obtained from overnight cultures after the appropriate dilution to allow at least 10 generations of growth in fresh medium before the temperature shifts. At the moment of the temperature shifts, the cultures had an A_{550} of between 0.02 to 0.04, and culture samples for microscopic analysis were taken at an A_{550} of between 0.25 and 0.45 (3, 4, and 5 h after the shift from the cultures at 39, 38, and 37°C, respectively).

Flow cytometry. Flow cytometry was essentially performed as described by Skarstad et al. (35). Samples from the bacterial cultures were collected, and the cells were directly fixed in ethanol by mixing 0.1 ml of a culture growing in M9 glucose medium with 1.75 ml of ice-cold 74% ethanol (70% ethanol [final concentration]). Fixed cells were stored at 4°C. For staining, 7.6×10^6 to 1.7×10^5 cells were pelleted by centrifugation. The cells were washed in 1 ml of cold staining buffer (10 mM Tris, pH 7.4; 10 mM $MgCl_2$), and after centrifugation the cells were carefully resuspended in 70 μl of the same buffer. An aliquot of the cell suspension (65 μl) was mixed with an equal volume of a staining solution (40 μg of ethidium bromide per ml and 200 μg of mithramycin A per ml, dissolved in the staining buffer). The analysis was performed with a Bryte HS flow cytometer using the software Win-Bryte version 1.06 (Bio-Rad). The measurements were carried out with the flow cytometer being triggered on light scattering. Thus, particles below a certain size were not recorded, and in this way it was possible to separate sample debris from small cells and the fluorescence of all particles above the threshold for light scattering was detected. Plastic calibration beads (Bio-Rad) with a diameter of 1.5 μm were used to monitor instrument performance and to standardize the scale for between-sample comparisons.

Cell size (light scattering) and DNA content (fluorescence) distributions obtained by flow cytometry were analyzed either directly (see Fig. 3 and 4) or after obtaining average values in the population for this parameters (see Fig. 2B and Table 1). To calculate the average cell size and DNA content values, the histogram curves were integrated by using the software Win-Bryte version 1.06.

Analysis of chromosome replication kinetics by flow cytometry. To analyze the kinetics of chromosome replication by flow cytometry, 200 μg of rifampin and 50 μg of cephalexin were added per milliliter to the cultures and samples were collected at different time points after addition of the drugs. Rifampin blocks the initiation of chromosome replication from *oriR1*, as well as from *oriC*, while allowing ongoing rounds of replication to be completed (9, 14). Cephalexin blocks cell division (7, 21). Addition of cephalexin to the cultures at the same time as rifampin allows a correct determination of the number of replication origins per cell (35). Inhibition of replication initiation, but not of elongation, results in cells containing fully replicated chromosomes after the replication runout. The DNA histograms will then display peaks corresponding to fully replicated chromosomes. Therefore, by flow cytometry it is possible to follow the appearance of peaks in the fluorescence histograms during the replication runout. In this way the speed of replication fork movement can be estimated (33, 34).

To compare the rates of chromosome replication progression of different cell populations, the evolution of the coefficients of variance for chromosome peaks during replication runout were analyzed. We determined the coefficients of variance (CVs) for the upper half of the peaks (CV-half values) corresponding to four chromosomes per cell, and these values versus the time of sampling were plotted. The curves showed two parts, a fast decrease in the beginning that was followed by a stabilization at a certain level of resolution. The values for the slope of the first part of the curves and the intersection point, in the *x* axis, between both parts of the curves were compared for the different populations under study (see Fig. 4B).

Microscopic studies. Cells, fixed in the same way as for flow cytometry analysis (70% ethanol [final concentration]) were pelleted and then resuspended in 0.9% NaCl. Aliquots (5 to 10 μl) were spread on microscope slides covered with thin layers of 1% agar containing 0.9% NaCl and 0.5 μg of 4′,6-diamidino-2-phenylindole (DAPI) per ml. With this staining technique, extensive nucleoid condensation and fusion are avoided (2, 37).

The cells were analyzed under a Nikon Optiphot-2 combined phase-contrast and fluorescence microscope. The images were digitalized by using a charge-

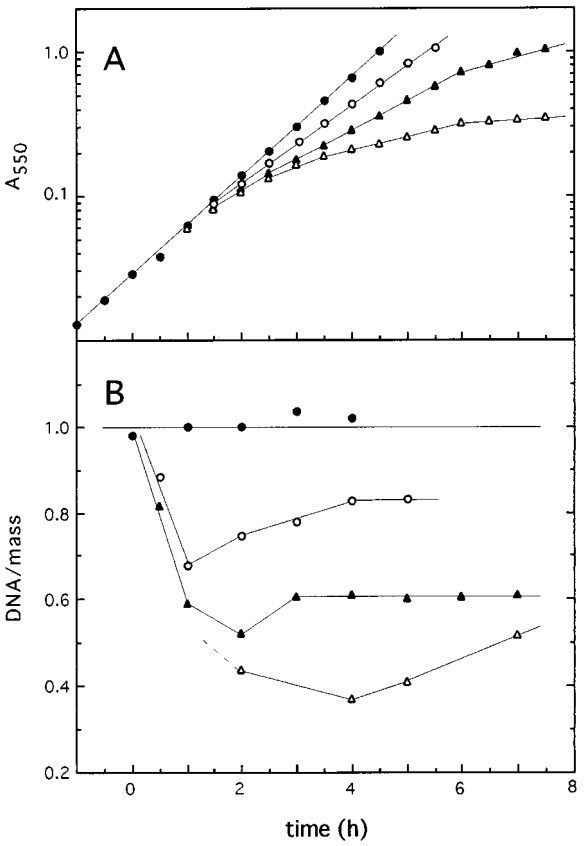

FIG. 2. Growth curves (A) and DNA/mass ratios (B) of EC::71CW/pOU420Ap^s. The strain was grown exponentially for at least 10 generations in M9 glucose medium at 39°C (●), and at time zero different parts of the culture were shifted to 38°C (○), 37°C (▲), or 36°C (△). The growth in mass was monitored by measuring absorbance (A_{550}), and the DNA/mass values were obtained from flow-cytometric measurements (see Materials and Methods). DNA/mass ratios are expressed relative to the values obtained at 39°C.

coupled device camera (Sony Instruments) connected to a computerized image analysis system (software and hardware from Bergström Instruments). Cell length measurements, analysis of septating cells, and determination of the number of nucleoids per cell were performed manually from the digitized images, using length measurement as well as profile tools provided with the software. The digitized images were transferred to Adobe Photoshop 3.0 and printed with a dye sublimation printer.

RESULTS

Underreplication levels during exponential growth. By decreasing the growth temperature of the *intR1* strain EC::71CW/pOU420Ap^s, it was possible to reduce its normal DNA/mass ratio, which at 39°C was close to that in the parental strain replicating from *oriC*, and to stabilize new ratios during a period of exponential growth.

EC::71CW/pOU420Ap^s and its *oriC* parental strain, EC1005, were grown exponentially in M9 glucose medium at 39°C for at least 10 generations. At an A_{550} of between 0.02 and 0.04, the cultures were split, and the parental strain was shifted to 37°C and the *intR1* strain was downshifted to 38, 37, or 36°C. The growth in mass was monitored by measuring the A_{550} (Fig. 2A; Table 1). Cells were collected from the cultures growing at 39°C and at different times after the temperature shift to 38, 37, or 36°C, fixed in ethanol, and analyzed by flow cytometry and microscopy (Fig. 2B and 3; Table 1) (see also Fig. 5). The DNA/mass ratios in the cultures at different incubation temperatures were estimated from the flow-cytometric data (Fig. 2B; Table 1).

The control strain, EC1005, had a mean doubling time ± standard deviation of 40 ± 2 min (n = 6) at 39°C, and the growth rate was essentially the same after the shift to 37°C (data not shown). Strain EC::71CW/pOU420Ap^s grew with a doubling time of 53 ± 2 min (n = 10) at 39°C. For more than 1 h after a temperature downshift, the culture's doubling time remained the same as it had been at 39°C; this was followed by a transition period during which the growth rate decreased. Then, the different cultures reached a new rate of exponential growth in mass. Thus, around 90 min after the shift to 38°C, the culture grew with a doubling time of about 66 ± 6 min (n = 7) for approximately three generations, and 140 min after the shift to 37°C, the culture reached 110 ± 30 min (n = 10) of doubling time, with that rate being maintained for about two cell generations (Fig. 2A; Table 1). Following the shift from 39 to 36°C, the culture did not undergo exponential growth for enough time to be analyzed systematically in the present study (Fig. 2A) (see also Fig. 6).

The DNA/mass ratio in EC::71CW/pOU420Ap^s was monitored after the temperature downshifts. Immediately after a shift, the DNA/mass ratio started to decrease, and it reached the minimum values of around 0.67 during the first hour after the shift to 38°C and of 0.52 2 h after the shift to 37°C. Then, an incrementation and stabilization of this ratio followed, with fairly constant levels of around 0.83 3 h after the shift to 38°C and of around 0.60 4 h after the shift to 37°C being reached (Fig. 2B; Table 1).

Flow-cytometric analysis showed that EC1005 and EC::71CW/pOU420Ap^s cultures growing exponentially at 39°C displayed similar cell size and DNA content distributions and average values (Fig. 3A). Three hours after the shift to 37°C, flow-cytometric distributions of EC1005 cultures were very similar to those seen during exponential growth at 39°C (data not shown). After the shift of EC::71CW/pOU420Ap^s to 37°C (Fig. 3B), the first effect that could be observed by flow cytometry was the reduction in the frequency of chromosome initiation, while the ongoing rounds of replication continued to comple-

TABLE 1. Physiological and cell division parameters for strain EC::71CW/pOU420Ap^s at different levels of replication[a]

Growth temp (°C)[a]	Doubling time (min)	DNA/mass (relative units)[b]	Mass/cell (relative units)[b]	Avg cell length (μm)[c]	Chromosomeless cells (%)[b]	Septation frequency (%)[c]	Avg length of septating cells (μm)[d]
39	53	1	1	3.10	5	10.47	5.03
38	66	0.83	1.16	3.95	7.5	9.27	6.16
37	110	0.60	1.65	8.12	20	4.85	10.08

[a] The values for all parameters were determined during exponential growth at 39°C (first line), 4 h after the shift to 38°C (second line), and 5 h after the shift to 37°C (third line) (cf. Fig. 2).
[b] Values were obtained by flow cytometry.
[c] A total of 1,000 cells in the population were analyzed.
[d] A total of 250 septating cells were measured.

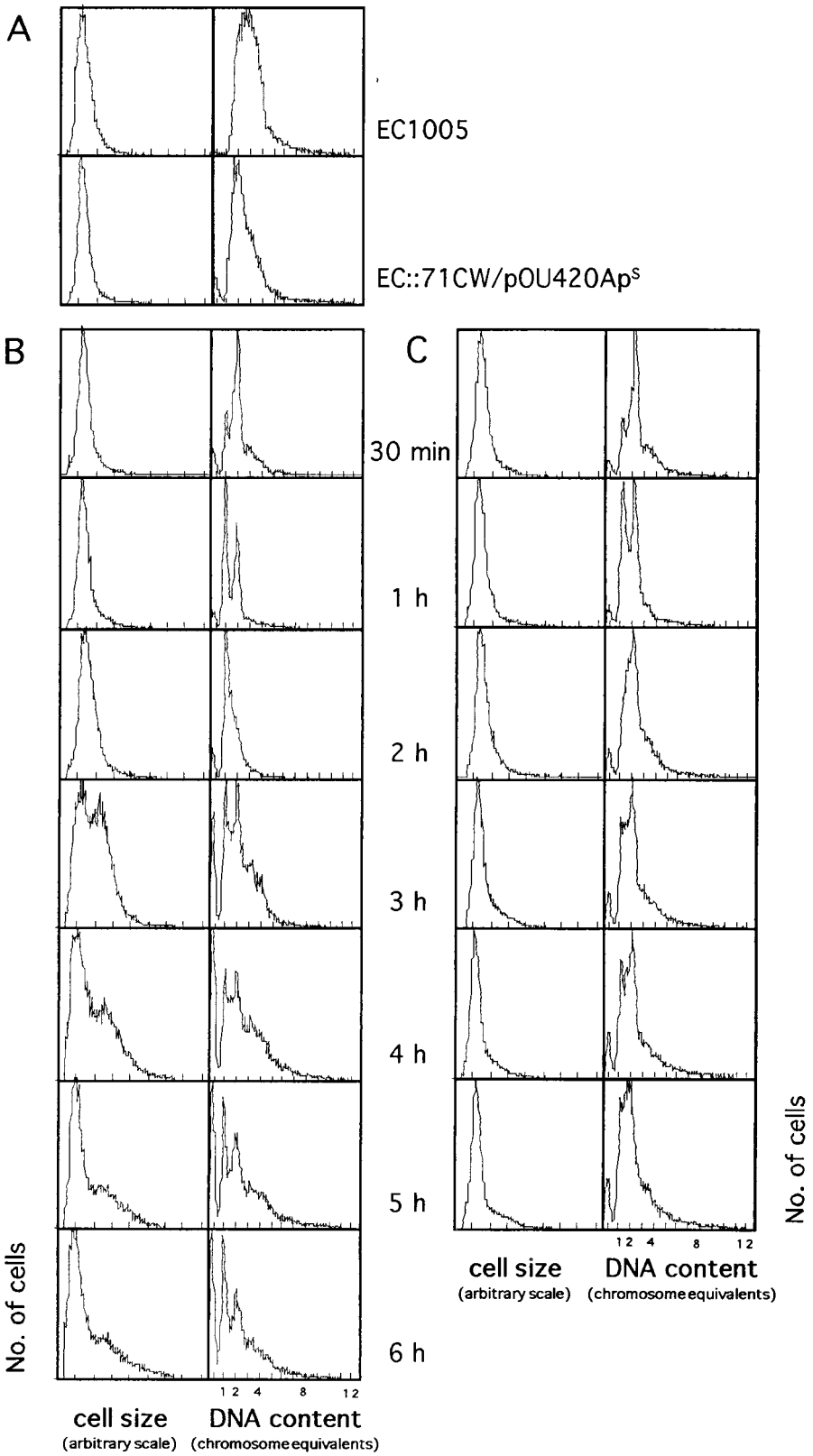

FIG. 3. Cell size (light scatter; left columns) and DNA content (fluorescence; right columns) distributions of EC1005 and EC::71CW/pOU420Ap^s growing exponentially in M9 glucose medium at 39°C (A) and of EC::71CW/pOU420Ap^s at different times after the shift to 37°C (B) or 38°C (C).

tion. This could be deduced from the appearance of distinct peaks in the DNA content distributions, corresponding to one and, mainly, to two (55% of the population) chromosome equivalents per cell, 30 min after the downshift. During the first hour after the shift, the cell size distribution and the average cell size, as well as the generation time of the culture (Fig. 2A), were constant; therefore, cell division took place as in the control situation. As a result of ongoing cell division, 1 h after the shift the fraction of cells with one chromosome became more abundant than that with two chromosomes. The rapid effect of the temperature downshift on replication could be ascribed to the sudden incrementation of the thermodependent production of CopA from the plasmid pOU420Ap^s as well as from the R1 copy present in the chromosome of the EC::71CW/pOU420Ap^s strain. Two hours after the shift, the majority of the cell population (56%) contained one chromosome, and it could be observed that replication resumed and some cells (25%) contained more than one chromosome but less than two. At this time, an initial effect on cell division could be detected because the cell size distribution got broader and the average size increased; thus, cell division started to be abolished. Three hours after the shift to 37°C, the doubling time for the culture increased (Fig. 2A) and replication resumed (Fig. 3B). Distinct peaks corresponding to cells with one, two, three, or four chromosomes could be distinguished instead of a more continuous distribution. The appearance of distinct peaks in the DNA content distribution indicated that a shorter period of time was spent on the replication process, relative to the whole cell cycle, at 37°C than at 39°C. The presence of a peak corresponding to cells that contained one chromosome confirmed that the temperature shift resulted in an increase in cell mass required for initiation of chromosome replication. At this stage, the percentage of chromosomeless cells started to increase. By this time, the cell size distribution shows two overlapping cell populations: one with a cell size corresponding to that of the culture growing at 39°C (45% of the population) and the other with a cell size approximately twice as big (55% of the population) as a result of cell division blockage.

After this transition period, a new state in the population was reached and held for the next 3 to 4 h (Fig. 3B, from 4 to 6 h). Replication continued at an underreplication level, as could be deduced from the presence in the population of a fraction of cells with an even lower DNA content than the cells with a low DNA content at 39°C. As time passed, the fractions of cells with no and one chromosome increased slowly in the population, each accounting for 20% of the total population 5 to 6 h after the temperature shifts (Fig. 3B; Table 1). Cell sizes were distributed in two overlapping populations, and whereas the small cells got slightly smaller than in the initial distribution, the bigger ones had a larger average cell size (see the average mass/cell ratios for the population in Table 1). The percentage of the smaller cells increased with time to represent around 60% of the population 5 to 6 h after the temperature shift. The distributions of the cell sizes and DNA contents were almost identical 5 and 6 h after the downshift. The distribution changed after 7 h, when the culture started to reach the stationary phase (data not shown). Hence, the inhibition of chromosome replication led to an abolishment of cell division, and the achievement of a new level of replication allowed cell division to resume.

In general, the effects on the cell population after the downshift to 38°C, as observed by flow cytometry, were essentially the same as those occurring after the shift to 37°C (Fig. 3C). However, the changes were less drastic and the new stable state was reached more quickly. The cell size distribution was similar to that at 39°C until 2 h after the shift. At later times, the cell population consisted of a majority of cells with the average cell size of the 39°C culture and a group of bigger cells; their proportions were 80 and 20%, respectively, 4 h after the shift (mass/cell ratios in Table 1). From the DNA content distribution, the same sequence of events as that occurring after the shift to 37°C could be observed; thus, replication resumed 2 h after inhibition of initiation of replication following the shift, and the new level was maintained during the following 3 h. In this case, when the population attained the new constant underreplication level, a percentage of the cell population with an even lower DNA content than the cells with a low DNA content in the 39°C culture could be detected, but the distribution did not present as distinct peaks as it had at 37°C. At the stable level, around 65% of the cell population contained from one to two chromosome equivalents per cell. In this case, the number of chromosomeless cells did not increase significantly, and thus the proportion moved from around 4.5% after the shift to around 7.5% after 4 h at 38°C (Fig. 3C; Table 1).

Since the proportion of chromosomeless cells increased in EC::71CW/pOU420Ap^s over time after the temperature shift down to 37°C, representing 20% of the population 5 h after the shift, the doubling time obtained by measuring the increment in absorbance in these cultures overestimates the real generation times (Table 1).

Replication speed during underreplication. The aim of the present work was to analyze the effects of a delay of the initiation of replication on cell division. Although a delay in the time of initiation of replication—that is to say, an increase in the average initiation mass—was detected by flow cytometry during periods of underreplication in EC::71CW/pOU420Ap^s after temperature downshifts (Fig. 3), a larger C/τ ratio could be an additional cause for the decrease in the DNA/mass ratio (10, 12). If an extension of the C period were the case, a delay in the time of cell division could be ascribed to the replication period being longer than in the control situation whenever a completed chromosome replication and correct partitioning are required for cell division. Hence, it was important to determine the length of the C period.

Addition of rifampin inhibits initiation of replication but allows ongoing replication to proceed to completion (runout replication) (see Materials and Methods). The kinetics of chromosome replication was determined by following the runout of chromosome replication by flow cytometry as described by Skarstad and Wold (34). Rifampin (200 μg/ml) and cephalexin (50 μg/ml) were added to EC::71CW/pOU420Ap^s cultures growing exponentially at 39°C and 5 h after the shift from 39 to 37°C. Samples for flow-cytometric analysis were collected at different time points after the addition of rifampin and cephalexin until the replication runout was completed. The replication kinetics for both situations were compared (Fig. 4). The amounts of time required for narrow peaks, representing fully replicated chromosomes, to appear were similar in the two cases. The DNA histograms of each culture showed that in both cases, the majority of the population contained fully replicated chromosomes 60 min after the addition of the drugs and that the best resolution was obtained at 120 min, when even peaks for more than four chromosomes per cell became defined (Fig. 4A). The resolution of the peaks corresponding to four chromosomes per cell at the two temperatures was analyzed by calculating the CV peaks (see Materials and Methods). The CV-half values versus the sampling time were plotted (Fig. 4B). The values of the slopes for the first part of the curves represent the speed of resolution, and the x values for the crossing point after extrapolation of both parts of the curve

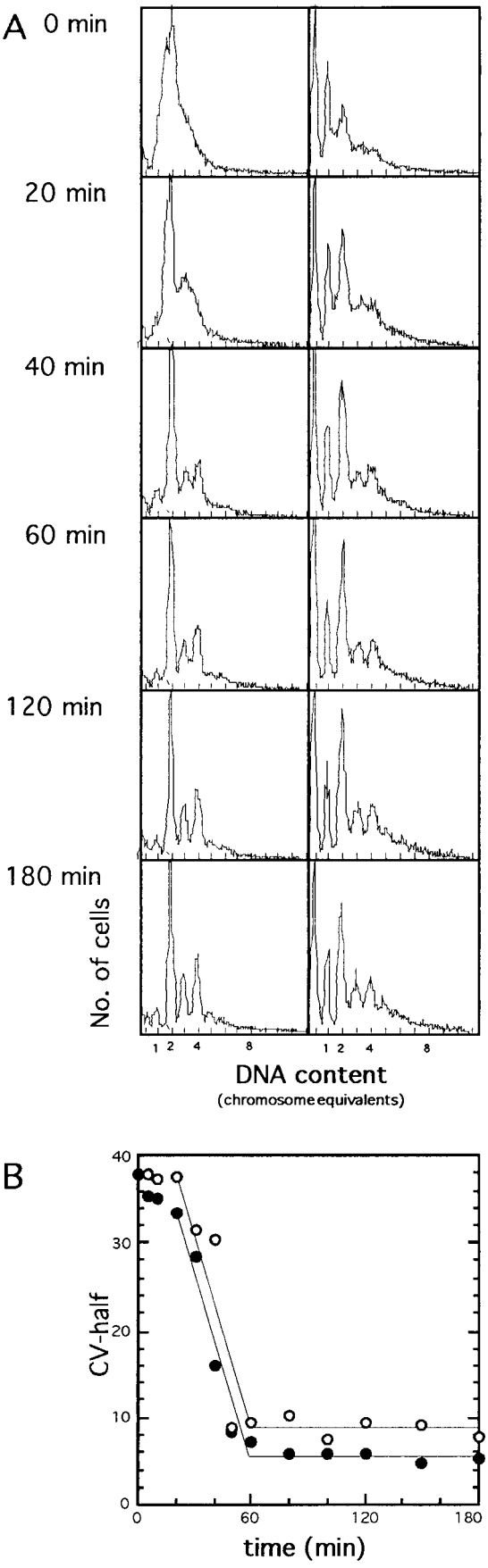

correspond to the time required for the resolution of the peak. The values obtained for the slopes were $-0.726\ min^{-1}$ at 39°C and $-0.794\ min^{-1}$ at 37°C, and the crossing point was at 57 min in both cases. Similar results were obtained in an analysis of the two-chromosome peaks (data not shown).

The similarity of the values for these parameters in the two situations indicates that the replication speed was approximately the same at 39°C and after the shift to 37°C. Therefore, this result ruled out any effect of the length of the C period on the decline in the DNA/mass ratio as well as on the cell division pattern under these conditions.

It should be noted that replication runout was more complete at 39°C than after the shift to 37°C, according to the resolution of the peaks in the DNA content distributions (Fig. 4A, 180 min); this effect was mainly observed in cells with more than three chromosome equivalents.

Cell division during underreplication. The effects of underreplication levels on cell division were studied in EC::71CW/pOU420Ap^s at different and stabilized DNA/mass ratios. With this analysis, we addressed two main questions regarding the control of cell division in bacteria: when and where cell division takes place.

Three hours after the temperature shifts from 39°C, 4 h after the shift to 38°C, and 5 h after the shift to 37°C, samples from the different cultures were collected and the cells were fixed in 70% ethanol. These cell populations were studied under the microscope after DAPI staining (see Fig. 5A). We analyzed 1,000 cells in the total population, or 250 cells in the case of septating cells, by phase-contrast and fluorescence microscopy and image analysis, and we determined the cell length, position of the incipient septum, and number of nucleoids per cell (see Materials and Methods).

Microscope images showed a homogeneous population of cells growing at 39°C, with an average normal cell size distribution and one or two nucleoids per cell (Fig. 5A, upper panel). After the temperature downshifts, the cell size and nucleoid distribution of the population became more heterogeneous. Cultures growing at 38 and 37°C 4 and 5 h after the shift, respectively, contained filamented cells as well as cells of normal size (Fig. 5A, middle and lower panels). At 38°C, many cells were slightly bigger than the average size at 39°C, and some filaments were present. The proportion of filamented cells in the population increased as the replication level decreased. Thus, at 37°C, many real filaments could be observed. Filamented cells frequently contained more than one or two nucleoids, generally having around four, which were clearly separated, and large DNA-free areas. At 37°C, DNA-less cells of normal size were frequently found. Therefore, the abolishment of cell division during underreplication that had been detected by flow cytometry was easily observed by microscopy (Fig. 3 and 5A; Table 1). This effect could be quantified by

FIG. 4. Kinetics of DNA synthesis during replication runout in EC::71CW/pOU420Ap^s. The strain was grown exponentially in M9 glucose medium at 39°C, and at an A_{550} of 0.029, part of the culture was shifted to 37°C. At an A_{550} of 0.29 at 39°C, and 5 h after the shift to 37°C (A_{550}, 0.28), rifampin (200 μg/ml) and cephalexin (50 μg/ml) were added to the cultures (time zero). At different time points, samples were collected and analyzed by flow cytometry. (A) DNA histograms during replication runout at 39°C (left column) and 5 h after the shift to 37°C (right column). The figure shows the distribution of DNA content in samples collected before (time zero) and at the indicated times after addition of the drugs. (B) Progress of the coefficient of variance (CV-half) for the four-chromosome peak during the runout of replication at 39°C (●) or 5 h after the shift to 37°C (○). Notice that more experimental data are taken into account in panel B than are shown in panel A.

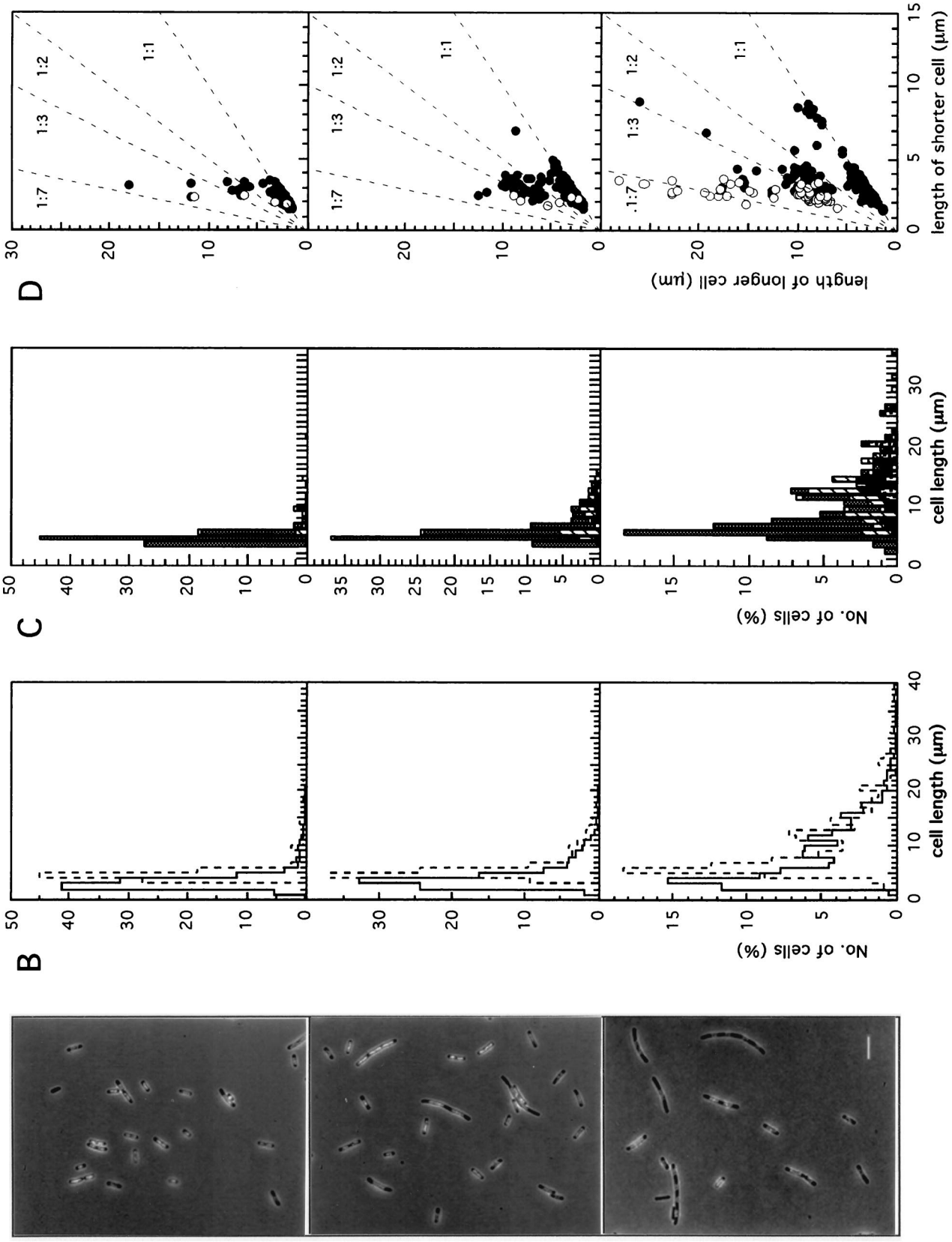

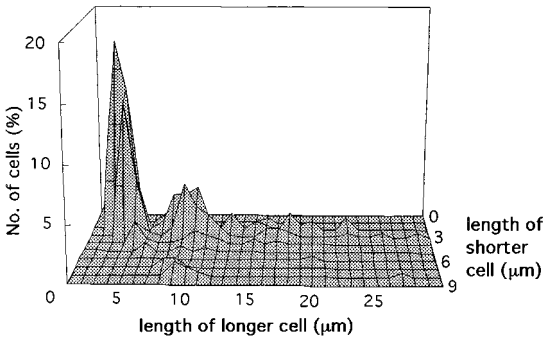

FIG. 6. Three-dimensional plot of the length of the two future daughter cells versus the number of cells obtained from length measurements of septating cells of EC::71CW/pOU420Ap^s growing at 37°C. The data are the same as in the lower panels Fig. 5B (broken lines) and 5D.

determining the increase of the average mass/cell ratio and cell length in the population (Table 1).

The frequency of cell division was determined by counting the number of septating cells among 1,000 cells from the total population. The septation frequency observed in exponentially growing cultures of EC::71CW/pOU420Ap^s with a normal DNA content was essentially maintained under moderate levels of underreplication (at 38°C). However, below some threshold level of replication (at 37°C), cell division was partially abolished and the frequency of septating cells was reduced (Table 1). The reduction in cell division frequency was also reflected in the increase of the average mass/cell ratio and cell length in the population (Table 1; Fig. 3 and 5A and B).

To determine when cells divide, the cell length of septating cells was measured (Fig. 5B). The distribution of the length of septating cells at 39°C showed a single peak, with a mean length ± standard deviation of 4.5 ± 0.7 μm (Fig. 5B, upper panel; Table 1, eighth column). After the shift to 38°C, the length distribution of the septating cells was essentially the same as that at the normal level of replication (at 39°C); thus, 80% of the cells were grouped around a mean length of 4.9 ± 0.8 μm, but the remaining 20% of the scored cells fell into a group with double the average length (10.0 ± 2.2 μm) (Fig. 5B, middle panel; Table 1). The cell length distribution of septating cells at 5 h after the shift to 37°C was clearly different from the situation at 39°C (Fig. 5B, lower panel). In this case, the distribution of cell length gave two distinct peaks, with average lengths of 6.5 ± 1.7 and 13.2 ± 1.6 μm for 63 and 25% of the scored cells, respectively. A minority of the cells, around 12%, were distributed in a more dispersed group with a mean length of 21.6 ± 4.5 μm. These distinct peaks are more easily seen in the three-dimensional plot shown in Fig. 6. The distinct peaks in the length distribution of septating cells at 37°C localized around one, two, and four times the length of the septating cells at 39°C, suggesting that if cell division cannot take place at the normal size, a discrete cell length (two or four times the normal cell size) is required to allow cell division.

By comparing the cell length distribution of septating cells to that of the total population in EC::71CW/pOU420Ap^s (Fig. 5B), the potentials for cell division for cells of the different lengths were compared. At 39°C, cells longer than the average population length were able to divide (Fig. 5B, upper panel). In the cases of underreplication, the main population divided with the same capacity as that observed at 39°C, but although they divided, the filamented cells had a reduced potential to carry out cell division (Fig. 5B, middle and lower panels); this is clear from the fact that the ratios between the two histograms are much higher at the cell length of normal dividing cells than at longer cell lengths.

The nucleoid distribution in septating cells was analyzed, and the numbers of nucleoids per cell for the different cell sizes are represented in Fig. 5C. At normal levels of replication, most of the dividing cells (around 90%) contained two nucleoids (Fig. 5C, upper panel). The fraction of septating cells with more than two nucleoids was increased as the level of replication decreased. Thus, after the temperature shift to 38°C, only 75% of the septating cells contained two nucleoids, and after the shift to 37°C, this proportion was diminished to 55% (Fig. 5C, middle and lower panels, respectively). The septating cells with two nucleoids had average lengths of 4.5, 5.2, and 7 μm at 39, 38, and 37°C, respectively. Septating cells containing more than two nucleoids were almost always longer than normal septating cells (Fig. 5C, lower panel); in these cells, the nucleoids were DNA masses well separated from each other. Therefore, no partitioning problems seem to cause abolishment of cell division during underreplication. This nucleoid distribution in septating cells can be considered as another result of the abolishment of cell division. Since the DNA/mass ratio in these populations was reduced, the fact that septating cells contained more than two nucleoids indicates that not only the completion of chromosome replication and partitioning but also a certain DNA/mass cell ratio is required to allow cell division.

To study the pattern of cell division during underreplication, the relative placement of the septa along the length axis of the cell was analyzed. The distance from each pole to the septum was measured for each cell, and the data were inserted in Fig. 5D. Despite the disturbance of the cell length at the time of septation, due to the abolishment of cell division during underreplication, the pattern of division septum localization in the elongated cells was nonrandom.

At normal levels of replication, when the septating cells were grouped in a single peak in the cell length distribution, the majority of the cells (around 94%) presented the incipient septum in the center of the cell, since they were grouped at around a 1:1 length ratio between the daughter cells (Fig. 5D, upper panel). In this case, a few daughter cells (0.8%) were chromosomeless. In the population growing for 4 h at 38°C after the shift from 39°C, 85% of the septating cells fell into the

FIG. 5. Phase-contrast and fluorescence photomicrographs (A), cell length distributions (B), septum localization patterns (C), and nucleoid distributions (D) for EC::71CW/pOU420Ap^s. The strain was grown exponentially in M9 glucose medium at 39°C, and at an A_{550} of between 0.02 to 0.04, the culture was split and downshifted to 38 and 37°C. Three hours after the shift from 39°C (upper panels), 4 h after the shift to 38°C (central panels), and 5 h after the shift to 37°C (low panels), cells from the cultures growing at the different temperatures were collected and fixed in ethanol (70%, final concentration). (A) After DAPI staining (0.5 μg/ml), the cell populations were analyzed by combined phase and fluorescence microscopy (see Materials and Methods). One thousand cells from the total population and 250 septating cells from each culture were analyzed. Bar, 5 μm. (B) Cell length distributions in the total population (continuous lines) and of septating cells (broken lines). (C) Septating cells with (from the top to the bottom of the bars) one (□), two (▨), three (▨), four (■), or five and more (▩) nucleoids. (D) To represent the localization of the septum, the lengths of the two future daughter cells produced in each septation event were plotted against each other, with the shorter cell always being chosen for the *x* axis. The dotted lines represent different daughter cell length ratios. Closed circles represent the cells which would give two nucleated daughter cells after division, and open circles represent the cells which would give one nucleated and one nucleoid-free daughter cell. In the latter case, the anucleate cell was always the shorter one.

1:1 length ratio class, but besides this, the septum was located in a one-quarter position in around 10% of the cells to give a 1:3 daughter length ratio (Fig. 5D, middle panel). In the 1:3 group, the shorter daughter cell had the normal length of a newborn cell. The frequency of chromosomeless cells after the shift to 38°C was essentially the same as that for the septating cells growing at 39°C (1.2% of the daughter cells). The effect of underreplication on the cell division pattern was more drastic after the shift to 37°C; the sizes of septating cells fell into distinct cell length classes. With regard to the septation pattern, two main groups could be clearly distinguished, corresponding to 1:1 and to 1:3 cell length ratios (Fig. 5D, lower panel). A reduced proportion of the septating cells belonged to the 1:1 group (60%), and instead an increased proportion of cells presented an asymmetric septation pattern; thus, in around 27% of the cells, the septation event produced a 1:3 daughter length ratio. A more dispersed group of cells, corresponding to 10% of the analyzed cells, could be ascribed to an 1:7 length ratio. The asymmetric septations always produced one daughter cell with about the same length as the shorter daughter cell formed at 39°C. Nevertheless, the length of the shorter cell slightly increased when the level of replication decreased; thus, the mean value for the length of the shorter cell, when considering only shorter cells smaller than 5 μm, increased from 2.2 ± 0.4 μm at 39°C to 2.5 ± 0.6 μm 4 h after the shift to 38°C and to 2.9 ± 0.7 μm 5 h after the shift to 37°C.

The cells with a central septum location (60%) could be divided into two groups: cells with a size similar to that at 39°C and a small cluster (4% of the total number of analyzed cells) with double-cell size in which the septum still formed in the middle position of the lengthwise cell axis. In the culture growing for 5 h at 37°C, chromosomeless cells represented 9% of the daughter cell population. The majority of cells which, after septation, would produce a chromosomeless daughter cell (96%) were located above the line of the 1:3 length ratio, and they accounted for 70% of the total cells in this area (Fig. 5D, lower panel). Therefore, the septation events which led to the production of one chromosomeless daughter cell took place in the longer cells, which still could form a visible septum, after an asymmetric septation; that is to say, when the shorter daughter cells came from the longer mother cells, they were almost always nucleoid free. Chromosomeless cells were always the shorter of the two cells produced after the septation event, and they had the same mean length as the shorter cell formed after the septation at 39°C (2.6 ± 0.5 μm for chromosomeless cells at 37°C, compared to 2.2 ± 0.4 μm for the shorter cell at 39°C).

Therefore, although cells with different lengths could divide, the septations at any level of replication resulted in a daughter cell length ratio of 1:1, 1:3, or 1:7. In no case was a cluster of cells found around the 1:2 length ratio. The proportions of cells at the different septation length ratios reflect a preference for central septations until a certain cellular length is reached. The frequency of the asymmetric septation increased as the level of replication decreased. It appears that when the delay in replication does not allow cell division at the normal cell length, asymmetric septations (1:3 and 1:7) begin to occur (Fig. 5D).

DISCUSSION

We have used a so-called *intR1* strain to vary the initiation mass of *E. coli* from normal to higher values by performing small changes in growth temperature. Shifting a culture growing exponentially at 39°C to 38 or 37°C resulted in a transition to new stable DNA/mass ratios, namely, about 80 and 60% of the initial value, respectively. This corresponds to a delay in the time of initiation of replication by 15 or 27% of the generation time (see below) (Fig. 1). Under these conditions, the septating cells were of two main classes, those that divided in the middle to give daughter cells of about normal size and those that were twice as big and divided to produce one daughter of normal size and one three times as big (1:3 ratio); some of the divisions resulted in one daughter (always the smallest) being chromosomeless. Our data are in accord with the mode denoted under-replication-II in Fig. 1. Under conditions of underreplication there was a considerable fraction of the cells that were elongated and contained more than two nucleoids. Hence, the direct coupling of nucleoid partitioning and cell division was lost. This suggests that cell division requires not only completed replication and nucleoid partitioning but also a DNA/mass ratio above a certain threshold value. Our main results, obtained under conditions of exponential growth, are similar to those reported by Bernander et al. (6) when cell division was studied after synchronous initiation of replication in the same *intR1* strain after runout of replication by shifting exponentially growing populations to 36°C.

It should be stressed that Fig. 1 gives an idealized picture of the cell cycle in *int* strains, since initiation of replication of the *intR1* chromosome is random over time (23); hence, the time of initiation varies within the population, but Fig. 1 describes the average situation. The randomness also explains why there was not a distinct shift from the normal cell division pattern to a new one during underreplication. There will always be some cells in which initiation of replication occurs early and that divide essentially normally.

The delay in initiation of replication caused by the transition from 39°C to 38 or 37°C can be calculated as follows. The average number of genome equivalents per cell, G, present in an exponentially growing population is determined by the equation $G = (\tau/C \cdot \ln 2)[2^{(C+D)/\tau} - 2^{D/\tau}]$ (11), in which C, D, and τ are the lengths of the C and D periods and the generation time, respectively. A delay by x min of initiation of replication would give the equation $G = (\tau/C \cdot \ln 2)[2^{(C+D-x)/\tau} - 2^{(D-x)/\tau}]$.

The values for the delay x cannot be calculated exactly because D is not known. However, the data from Fig. 4 show that the lengths of the C period at 39 and 37°C were approximately the same. Hence, assuming that C and D are 57 (Fig. 4) and 20 min, respectively, the value of x can be calculated to be 10 and 30 min at 38 and 37°C, respectively, or 15 and 27% of the generation times at these two temperatures. It should also be stressed that the measured generation times are overestimates of the real ones because DNA-less cells were formed during underreplication.

During underreplication, the cell length distributions of the septating cells were slightly broader than under normal conditions; this broadening took place only at the large side of the cell length distributions. This indicates that cell division could be postponed when replication and nucleoid partitioning were slightly delayed and that when the delay were longer, cell division would be omitted and would not take place until one doubling in mass later (Fig. 5D). The molecular nature of this putative cross talk between replication-nucleoid partitioning and cell division is unknown. Previous experiments showed that the SOS- and SfiA-mediated division inhibition was not the main reason for the cessation of division that was observed after runout of chromosome replication in this *intR1* strain (6). Under these conditions, some of the divisions occurred at twice the normal mother length; in this case, one of the daughter cells was of normal newborn size. This favors the idea that cell division has got its own, independent control system. It had been expected that the cells would divide in the middle. The

1:3 division pattern of elongated cells suggests that there is a size window during which cell division is allowed. The maximum size that still allowed cell division was about 25% bigger than the maximum size of dividing cells at the normal DNA/mass ratio (Fig. 5D). If cell division has not occurred at this size, it is omitted and a second opportunity occurs one mass doubling later. However, the ability to divide in the middle is lost, and cell division now takes place at new sites one-fourth of the cell length from the poles. Hence, cell division in some way seems to measure the distance from one of the poles; according to Donachie et al. (16), cell division at all growth rates initiates at a specific cell length rather than at a specific cell mass. As a matter of fact, even when very long cells divided, one of the daughters was of normal cell size, and although the number of measured cells was small, our data suggest that division occurs at a 1:7 ratio between the lengths of the two daughter cells. It may be appropriate to mention that Raskin and de Boer (31) showed that the MinE protein forms a ring in the middle of the cell very early in the cell cycle. They found that there were two MinE rings in some elongated cells and that these rings were placed one-fourth of the cell length from each cell pole, as if the ring in the middle had disappeared. As a matter of fact, we observed that filamented cells occasionally contained two septa at the cell quarters, with the normal distance to each pole, and that only about 4% of the septating cells at 37°C were twice the normal mother size and still divided in the middle.

Omission of one cell division led to the appearance of elongated cells with more than two separated nucleoids. Hence, there was no tight coupling between completed replication-nucleoid partitioning and cell division; rather, for cell division to occur, not only must cells be of an appropriate size and two separated nucleoids be present, but also the DNA/mass ratio must be above a certain threshold value.

During underreplication, in a significant number of divisions of filamented cells the smallest daughter did not contain chromosomal DNA. Several groups have studied the cell size distribution of anucleate cells formed after total inhibition of DNA replication by using temperature-sensitive *dna* strains (20, 22, 25, 26, 36). The data are somewhat conflicting; some groups found that the anucleate cell size distribution was narrow and comparable to that of normal newborn cells (22, 36), whereas Mulder and Woldringh (25, 26) reported a more random distribution. In our case, the anucleate daughter cells were of normal size, supporting the idea of a nonrandom positioning of the septa (see also reference 20, p. 1635 to 1636). We have earlier favored the idea that the size of the nucleoid determines the size of the daughter cells (2), but the size of the DNA-less cells contradicts this and strengthens the conclusion that cell division has its own control system also with respect to the position of the division site.

When *E. coli* is grown in different media its generation time varies. The dimensions of the cells, both diameter and length, increase with increasing growth rate (16, 39). In the present study, however, although there was a reduction in growth rate during underreplication, the cell diameter did not change measurably (0.84 ± 0.08 μm at 39°C versus 0.88 ± 0.09 μm at 37°C) (Fig. 5A). Hence, it appears that the diameter of the cells is set by the medium rather than by the growth rate.

In conclusion, our studies with *intR1* strains under conditions of both overreplication (3) and underreplication (this paper) indicate that cell division has its own control system, with respect both to its coupling to the cell mass and to the positioning of the division sites, that is independent of chromosome replication. The nature of this control system is not yet known.

ACKNOWLEDGMENTS

This work was supported by the Swedish Natural Science Research Council and the Swedish Cancer Society. Grants from the Knut and Alice Wallenberg foundation enabled us to purchase the microscope and the image analysis equipment. E.B. acknowledges a fellowship from the Swedish Institute.

REFERENCES

1. **Åkerlund, T., K. Nordström, and R. Bernander.** 1993. Branched *Escherichia coli* cells. Mol. Microbiol. **10:**849–858.
2. **Åkerlund, T., R. Bernander, and K. Nordström.** 1992. Cell division in *Escherichia coli minB* mutants. Mol. Microbiol. **6:**2073–2083.
3. **Bernander, R., and K. Nordström.** 1990. Chromosome replication does not trigger cell division in *E. coli*. Cell **60:**365–374.
4. **Bernander, R., A. Merryweather, and K. Nordström.** 1989. Overinitiation of replication of the *Escherichia coli* chromosome from an integrated runaway-replication derivative of plasmid R1. J. Bacteriol. **171:**674–683.
5. **Bernander, R., S. Dasgupta, and K. Nordström.** 1991. The *E. coli* cell cycle and the plasmid R1 replication cycle in the absence of the DnaA protein. Cell **64:**1145–1153.
6. **Bernander, R., T. Åkerlund, and K. Nordström.** 1995. Inhibition and restart of initiation of chromosome replication: effects on exponentially growing *Escherichia coli* cells. J. Bacteriol. **177:**1670–1682.
7. **Boye, E., and A. Løbner-Olesen.** 1991. Bacterial growth control studied by flow cytometry. Res. Microbiol. **142:**131–135.
8. **Bramhill, D., and A. Kornberg.** 1988. Duplex opening by dnaA protein at novel sequences in initiation of replication at the origin of *E. coli* chromosome. Cell **52:**743–755.
9. **Bremer, H., and G. Churchward.** 1977. Deoxyribonucleic acid synthesis after inhibition of initiation of rounds of replication in *Escherichia coli* B/r. J. Bacteriol. **130:**692–697.
10. **Churchward, G., E. Estiva, and H. Bremer.** 1981. Growth rate-dependent control of chromosome replication initiation in *Escherichia coli*. J. Bacteriol. **145:**1232–1238.
11. **Collins, J., and R. H. Pritchard.** 1973. Relationship between chromosome replication and F′lac episome replication in *Escherichia coli*. J. Mol. Biol. **78:**143–155.
12. **Cooper, S., and C. E. Helmstetter.** 1968. Chromosome replication and the division cycle of *Escherichia coli* B/r. J. Mol. Biol. **31:**519–540.
13. **Dasgupta, S., R. Bernander, and K. Nordström.** 1991. In vivo effect of the *tus* mutation on cell division in an *Escherichia coli* strain where chromosome replication is under the control of plasmid R1. Res. Microbiol. **142:**177–180.
14. **Díaz, R., K. Nordström, and W. L. Staudenbauer.** 1981. Plasmid R1 replication dependent on protein synthesis in cell-free extracts of *E. coli*. Nature **289:**326–328.
15. **Donachie, W. D.** 1993. The cell cycle of *Escherichia coli*. Annu. Rev. Microbiol. **47:**199–230.
16. **Donachie, W. D., K. J. Begg, and M. Vicente.** 1976. Cell length, cell growth and cell division. Nature **264:**328–333.
17. **Eliasson, Å., K. Nordström, and R. Bernander.** 1996. *Escherichia coli* strains in which chromosome replication is controlled by a P1 or F replicon integrated into *oriC*. Mol. Microbiol. **20:**1013–1023.
18. **Engberg, B., and K. Nordström.** 1975. Replication of R-factor R1 in *Escherichia coli* K-12 at different growth rates. J. Bacteriol. **123:**179–186.
19. **Grinsted, J., J. R. Saunders, L. C. Ingram, R. B. Sykes, and M. H. Richmond.** 1972. Properties of an R factor which originated in *Pseudomonas aeruginosa* 1822. J. Bacteriol. **110:**529–537.
20. **Helmstetter, C. E.** 1996. Timing of synthetic activities in the cell cycle, p. 1627–1639. *In* F. C. Neidhardt, R. Curtiss III, J. L. Ingraham, E. C. C. Lin, K. B. Low, B. Magasanik, W. S. Reznikoff, M. Riley, M. Schaechter, and H. E. Umbarger (ed.), *Escherichia coli* and *Salmonella*: cellular and molecular biology, 2nd ed., vol. 2. ASM Press, Washington, D.C.
21. **Ishino, F., and M. Matsuhashi.** 1981. Peptidoglycan synthetic enzyme activities of highly purified penicillin-binding protein 3 in *Escherichia coli*: a septum-forming reaction sequence. Biochem. Biophys. Res. Commun. **101:**905–911.
22. **Jaffé, A., R. D'Ari, and V. Norris.** 1986. SOS-independent coupling between DNA replication and cell division in *Escherichia coli*. J. Bacteriol. **165:**66–71.
23. **Koppes, L., and K. Nordström.** 1986. Insertion of an R1 plasmid into the origin of replication of the *E. coli* chromosome: random timing of replication of the hybrid chromosome. Cell **44:**117–124.
24. **Lutkenhaus, J., and A. Mukherjee.** 1996. Cell division, p. 1615–1626. *In* F. C. Neidhardt, R. Curtiss III, J. L. Ingraham, E. C. C. Lin, K. B. Low, B. Magasanik, W. S. Reznikoff, M. Riley, M. Schaechter, and H. E. Umbarger (ed.), *Escherichia coli* and *Salmonella*: cellular and molecular biology, 2nd ed., vol. 2. ASM Press, Washington, D.C.
25. **Mulder, E., and C. L. Woldringh.** 1989. Actively replicating nucleoids influence positioning of division sites in *Escherichia coli* filaments forming cells lacking DNA. J. Bacteriol. **171:**4303–4314.
26. **Mulder, E., and C. L. Woldringh.** 1991. Autoradiographic analysis of diaminopimelic acid incorporation in filamentous cells of *Escherichia coli*: re-

pression of peptidoglycan synthesis around the nucleoid. J. Bacteriol. **173:** 4751–4756.
27. **Murray, A., and T. Hunt.** 1993. The cell cycle: an introduction. Oxford University Press, Inc., New York, N.Y.
28. **Nordström, K., and E. G. H. Wagner.** 1994. Kinetic aspects of control of plasmid replication by antisense RNA. Trends Biochem. Sci. **19:**294–300.
29. **Nordström, K., R. Bernander, and S. Dasgupta.** 1991. Analysis of the bacterial cell cycle using strains in which chromosome replication is controlled by plasmid R1. Res. Microbiol. **142:**181–188.
30. **Nordström, K., R. Bernander, and S. Dasgupta.** 1991. The *Escherichia coli* cell cycle: one cycle or multiple independent processes that are co-ordinated? Mol. Microbiol. **5:**769–774.
31. **Raskin, D. M., and P. A. de Boer.** 1997. The MinE ring: an FtsZ-independent cell structure required for selection of the correct division site in *E. coli*. Cell **91:**685–694.
32. **Sambrook, J., E. F. Fritsch, and T. Maniatis.** 1989. Molecular cloning: a laboratory manual, 2nd ed. Cold Spring Harbor Laboratory Press, Cold Spring Harbor, N.Y.
33. **Skarstad, K., A. Løbner-Olesen, T. Atlung, K. von Meyenburg, and E. Boye.** 1989. Initiation of DNA replication in *Escherichia coli* after the overproduction of the DnaA protein. Mol. Gen. Genet. **218:**50–56.
34. **Skarstad, K., and S. Wold.** 1995. The speed of the *Escherichia coli* fork in vivo depends on the DnaB:DnaC ratio. Mol. Microbiol. **17:**825–831.
35. **Skarstad, K., R. Bernander, S. Wold, H. B. Steen, and E. Boye.** 1994. Cell cycle analysis of microorganisms, p. 241–255. *In* M. Al-Rubeai and A. N. Emery (ed.), Flow cytometry applications in cell culture. Marcel Dekker Inc., New York, N.Y.
36. **Tang, M.-S., and C. E. Helmstetter.** 1980. Coordination between chromosome replication and cell division in *Escherichia coli*. J. Bacteriol. **141:**1148–1156.
37. **Van Helvoort, J. M. L. M., J. Kool, and C. L. Woldringh.** 1996. Chloramphenicol causes fusion of separated nucleoids in *Escherichia coli* K-12 cells and filaments. J. Bacteriol. **178:**4289–4293.
38. **Vinella, D., and R. D'Ari.** 1995. Overview of controls in the *Escherichia coli* cell cycle. Bioessays **17:**527–536.
39. **Zaritsky, A.** 1975. On dimensional determination of rod-shaped bacteria. J. Theor. Biol. **54:**243–248.